Electron-impact excitation of the $6p7s\ ^3P_1$ state of Pb atom at small scattering angles

S. Milisavljević,[1] M. S. Rabasović,[1] D. Šević,[1] V. Pejčev,[1,2] D. M. Filipović,[1,3] Lalita Sharma,[4] Rajesh Srivastava,[4] A. D. Stauffer,[5] and B. P. Marinković[1]

[1]*Institute of Physics, Pregrevica 118, 11080 Belgrade, Serbia*

[2]*Faculty of Natural Sciences, Radoja Domanovića 12, 34000 Kragujevac, Serbia*

[3]*Faculty of Physics, University of Belgrade, P. O. Box 368, 11001 Belgrade, Serbia*

[4]*Department of Physics, Indian Institute of Technology, Roorkee 247667, India*

[5]*Department of Physics and Astronomy, York University, Toronto, Canada M3J 1P3*

(Received 16 March 2007; published 18 May 2007)

Electron-impact excitation of the $6p7s\ ^3P_1$ state of Pb atom has been investigated both experimentally and theoretically. Differential cross sections (DCSs) were measured at incident electron energies of $E_0=10$, 20, 40, 60, 80, and 100 eV and small scattering angles up to 10° using a crossed electron-atom beam technique. The forward scattering function method has been used for determination of the absolute generalized oscillator strengths and DCS values. Corresponding relativistic distorted wave calculations have been performed and compared with experimental results.

DOI: 10.1103/PhysRevA.75.052713 PACS number(s): 34.80.Dp

I. INTRODUCTION

Electron-impact excitation of Pb atoms is of both applied and fundamental interest. Many plasma diagnostic and modeling techniques require electron-impact excitation cross sections as input data for the calculation of plasma parameters. Besides this, detailed electron-atom collision data are very important in astrophysics. They are essential for identifying electron-impact excited lines in spectra of various astrophysical objects including stars and interstellar gas clouds and therefore have a critical role in abundance analysis and chemical composition determination of these objects [1–4].

Growing interest in reliable e/Pb collision data stimulated this research in electron atom scattering processes. In this open-shell atom with high Z value, relativistic effects are expected to play an important role. Unfortunately, there are only a few experimental and theoretical investigations related to the electron excitation of the Pb atom. Williams and Trajmar [5] presented experimental differential and integral cross sections for the excitation of the first five states at single incident electron energy of 40 eV. The theoretical study by Bartschat [6] was concerned with elastic and inelastic electron scattering in the energy range up to 7 eV. Using the semirelativistic R-matrix method he calculated total electron-impact cross sections for the transitions from the ground $6p^2\ ^3P_0$ state to the $6p^2\ ^3P_{0,1,2}$, $^1D_2$, and $^1S_0$ states. The main motivation for the calculation by Wijesundra *et al.* [7] was to reinvestigate the structure of the Pb atom and to calculate cross sections for the elastic scattering and electron-impact excitation of the four lowest-lying excited states. The results were obtained using the Dirac R-matrix method in the energy range from 0 to 4 eV. The authors also presented resonance structures. In comparison with the previous R-matrix calculation of Bartschat [6] they found disagreement between calculated positions of the resonance structures which probably results from the different methods used to account for relativistic effects. Kaur *et al.* [8] reported relativistic distorted wave (RDW) results for differential cross sections (DCSs) for the electron impact excitation of lead for the fine-structure transitions $^3P_0-^3P_1$, $^3P_2$ and $^1D_2$, and for all of the generalized polarization parameters in the energy range from 11 to 40 eV. The calculation includes both the fine structure of the atom and the spin orbit coupling of the scattered electrons. The previous measurements using polarized electrons include work by Geesmann *et al.* [9]. They have developed an experimental apparatus for studying both elastic and inelastic transitions that allowed them to measure the left-right asymmetry of polarized electrons scattered from unpolarized targets at energies below 6 eV. Recently, data for lead atom excited to the resonant $6p7s\ ^3P_1$ state by polarized electron impact were reported by Herting *et al.* [10]. The results are obtained using the electron-photon coincidence technique and are compared with the semirelativistic Breit-Pauli R-matrix and RDW calculations.

This experiment extends our previous work on Pb [11,12] by providing new scattering data for lead atoms. Here we present results of a joint experimental and theoretical investigation of electron-lead excitation. Inelastic collisions leading to excitation of the $6p7s\ ^3P_1$ level from the $6p^2\ ^3P_0$ ground state have been studied experimentally at incident electron energies of 10, 20, 40, 60, 80, and 100 eV and scattering angles from 1° to 10°. We report absolute generalized oscillator strengths (GOS) for the $6p^2\ ^3P_0 \rightarrow 6p7s\ ^3P_1$ transition in Pb and corresponding DCS values. These absolute GOSs and DCSs are determined through normalizations to the optical oscillator strength using the forward scattering function method. Relativistic distorted wave calculations of electron-lead scattering were performed and are compared with the experimental data.

II. EXPERIMENTAL TECHNIQUE AND PROCEDURES

The new inelastic scattering data for Pb atom excited to the $6p7s\ ^3P_1$ state by electron impact are obtained using the same experimental setup as for the Ca, Zn, and Mg experiments [13–15]. In these references a more detailed description of the apparatus and operating conditions has been presented, therefore only a brief summary will be given here.

The experiment was carried out using a crossed electron-atom beam technique in the electron spectrometer "ESMA." The monoenergetic beam of electrons from the monochromator was perpendicularly crossed by the atomic beam. A lead vapor beam was produced by heating an oven crucible (aspect ratio $\gamma=0.075$) containing Pb metal by two separate heaters which provided a variable temperature difference between the top and bottom—the nozzle was maintained at approximately 100 K higher temperature in order to prevent clogging. The working temperature was about 1170 K and background pressure was of the order of 10^{-5} Pa. A double μ-metal magnetic shield reduced the Earth's magnetic field to less than 10^{-7} T in the chamber.

The energy scale was calibrated by measuring the position of the feature in the elastic scattering attributed to the threshold energy of the $6p7s\ ^3P_1$ state of Pb at 4.375 eV. This resonance structure is clearly resolved with an overall system energy resolution [full width at half maximum (FWHM)] of about 120 meV. The angular resolution was estimated to be 1.5°. Scattered electron intensity was measured as a function of scattering angle by a hemispherical electron energy analyzer and channel electron multiplier as a single-electron detector. The analyzer can be positioned from −30° to 150° with respect to the incoming electron beam.

The measurement procedure included several steps. Before each measurement the energy loss spectra were recorded to verify the absence of double scattering. Then the angular distribution of the scattered electrons was measured at small scattering angles. The position of the true zero angle was determined and checked according to the symmetry of scattering intensities at negative and positive angles between −10° and +10°. Effective path length correction factors [16] adopted for our scattering geometry and experimental conditions convert the measured intensities to relative differential cross sections. In order to put our results on an absolute scale, following the method described by Felfli and Msezane [17], we normalized the relative DCSs by using the forward scattering function (FSF) introduced by Avdonina *et al.* [18]. It is well known that accurate DCS values for optically allowed transitions at small scattering angles are difficult to obtain, particularly at high impact energies when DCSs increase dramatically as the scattering angle approaches to zero. One of the most used techniques for normalization consists of extrapolating the measured DCSs data down to zero momentum transfer through the unphysical region of scattering angles [19]. Including the limiting behavior of the generalized oscillator strength (GOS) which tends to optical oscillator strength (OOS) as the square of the momentum transfer (K^2) tends to zero and using the known OOS value for some optically allowed transition, Avdonina *et al.* [18] introduced the FSF and obtained GOS values for this transition for forward electron scattering at small momentum transfer without traversing the unphysical region. Following this theoretical approach which uses only the OOS as input, it is applicable for $E_0 \geq 2.5\omega$ (where ω is excitation energy), and it ensures successful connection of experimental GOS results with corresponding OOS. Felfli and Msezane [17] utilized this procedure for normalizing the measured relative DCSs through the GOSs over a wide range of the electron impact energies. Due to this procedure, for a given E_0, the smallest value of K^2 was obtained for zero scattering angle. Since this value corresponds to absolute GOS for forward scattering which lies on the FSF curve, extrapolated and properly normalized relative GOSs must terminate on the FSF curve exactly at this point. Also, in appropriate representation the GOS varies linearly with K^2 for small scattering angles and linearity decreases as E increases away from threshold. In this work we generated the FSF curve using the OOS value of 0.21 taken from the NIST database [20]. This value is somewhat larger than recommended value of 0.19 ± 0.02 by Doidge [21] but smaller than the obtained value of 0.26 by Biemont *et al.* [22]. Relative DCSs ($\mathcal{C}$) were converted to the generalized oscillator strengths ($\mathcal{S}$) according to the following formula:

$$\mathcal{S}(K,E) = \frac{\omega}{2}\frac{k_i}{k_f}K^2\mathcal{C}(E,\theta), \tag{1}$$

where ω is excitation energy, k_i and k_f are the electron momenta before and after the collision, and the momentum transfer K is defined by

$$K^2 = 2E\left[2 - \frac{\omega}{E} - 2\sqrt{1-\frac{\omega}{E}}\cos\theta\right], \tag{2}$$

where E is the impact energy. The GOS values obtained were fitted and extrapolated from the small values of K^2 obtained from zero scattering angle data and normalized to the FSF. These normalization factors were then used to obtain absolute DCS values.

III. CALCULATION METHOD

In the RDW method the transition matrix for the electron impact excitation of an atom having N electrons from an initial state i to a final state f is given by (atomic units are used throughout)

$$T_{i\to f}^{\mathrm{DW}} = \langle \chi_f^-(1,2,\ldots,N+1)|V - U_f(N+1)|A\chi_i^+(1,2,\ldots,N+1)\rangle, \tag{3}$$

where V is the target-projectile interaction and U_f is the distortion potential which is taken to be a function of the radial coordinates of the projectile electron only. U_f is chosen to be a spherically averaged static potential of the final state of the atom.

The wave functions $\chi_{\mathrm{ch}}^{+(-)}$, where "ch" refers to the two channels, i.e., initial "i" and final "f," are represented as a product of the N-electron target wave functions ϕ_{ch} and a projectile electron distorted wave function $F_{i(f)}^{\mathrm{DW}+(-)}$, i.e.,

$$\chi_{\mathrm{ch}}^{+(-)}(1,2,\ldots,N+1) = \phi_{\mathrm{ch}}(1,2,\ldots,N)F_{\mathrm{ch}}^{\mathrm{DW}+(-)}(\mathbf{k}_{\mathrm{ch}},N+1). \tag{4}$$

Here "+" refers to an outgoing wave, while "−" denotes an incoming wave. A is the antisymmetrization operator that takes into account the exchange of the projectile electron with the target electrons and $\mathbf{k}_{\mathrm{ch}}$ are the linear momenta of the projectile electron in the initial and final state. The distorted waves F are solutions of the Dirac equations including

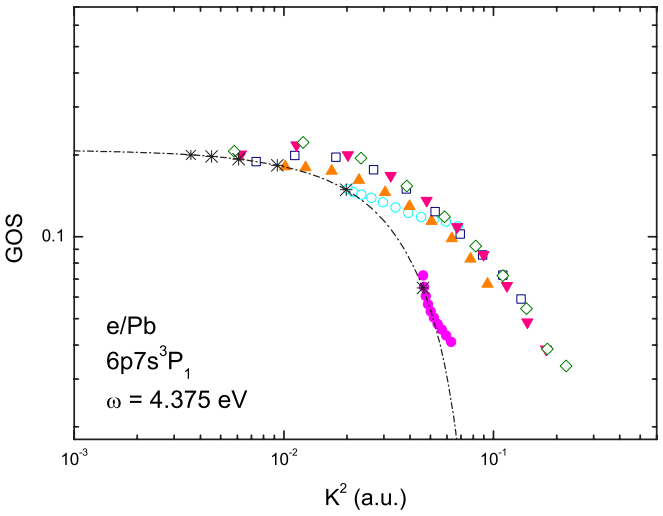

FIG. 1. (Color online) Generalized oscillator strengths (GOS) for the $6p7s\ ^3P_1$ state of lead atoms versus momentum transfer squared (K^2) at 10 (filled circles), 20 (open circles), 40 (filled up triangles), 60 (open squares), 80 (filled down triangles), and 100 eV (open diamond) electron-impact energies. Stars show the appropriate minimal values of K^2 and the dash-dotted line represents the forward scattering function (FSF) generated using the optical oscillator strength (f) value of 0.21.

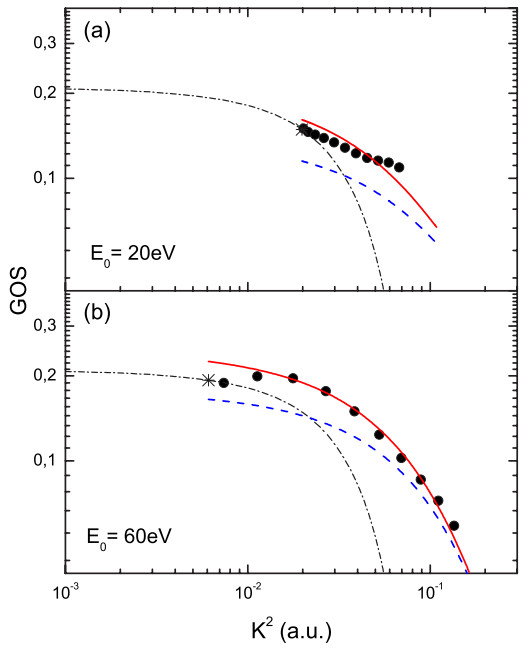

FIG. 2. (Color online) Generalized oscillator strengths (GOS) for the $6p7s\ ^3P_1$ state of lead versus momentum transfer squared (K^2) at (a) E_0=20 eV and (b) E_0=60 eV electron-impact energies. Filled circles denote the present experimental results, the solid line denotes MCGS calculations, and the dashed line denotes SCGS calculations. Stars indicate the appropriate minimal values of K^2, while the dash-dotted line represents the forward scattering function (FSF).

the distortion potential U_f and depend on the spin of the projectile electron. More details are given in Chauhan *et al.* [23], where we studied electron impact excitation of the ground state of calcium.

Since our calculations are carried out in the relativistic j-j coupling scheme the wave functions $\phi_{\rm ch}$ have a definite total angular momentum and the spin of the projectile electron is specified. Thus we can write the T-matrix in the alternate form

$$T_{i\to f}^{\rm DW} = \langle J_f M_f \mu_f | V - U_f | J_i M_i \mu_i \rangle, \tag{5}$$

where J and M represent the total angular momentum of the atomic state and μ is the spin projection of the free electron. With our normalization of the distorted waves, the differential cross section for the excitation of the atom from the initial state metastable level with angular momentum J_i to a higher lying level J_f is given by

$$\mathrm{DCS} = (2\pi)^4 \frac{k_f}{2(2J_i+1)k_i} \sum_{M_i M_f \mu_i \mu_f} |\langle J_f M_f \mu_f | V - U_f | J_i M_i \mu_i \rangle|^2, \tag{6}$$

where we have summed over the spins of the incident and scattered electron since these are not observed in the experiment.

The ground state of Pb is a fine-structure level of the $6p^2$ valence shell with J=0. We are considering the excitation of this state to the $6s7p\ ^3P_1$ level. Thus we have J_i=0 and J_f=1. Since we are working in the j-j coupling scheme we represent the p electrons as $\bar{p}$ with total angular momentum j=1/2 and p with j=3/2. We have used two different sets of wave functions in our calculations which are determined from the GRASP92 program of Parpia *et al.* [24]. The first, labeled SCGS (single-configuration ground state), uses the minimal spectroscopic configurations for the initial and final states. In this case we have

$$\phi_i = a_1(6\bar{p}^2)_{J=0} + a_2(6p^2)_{J=0} \tag{7}$$

and

$$\phi_f = b_1(6\bar{p}7s)_{J=1} + b_2(6p7s)_{J=1}, \tag{8}$$

with a_1=0.960 148, a_2=−0.279 49, b_1=0.99 734, and b_2=0.072 88. This yields an optical oscillator strength of 0.167 96. The second set, labeled MCGS (multiconfiguration ground state), involves more elaborate wave functions obtained by adding additional configurations to the basic set. These are given by

$$\phi_i = a_1(6\bar{p}^2)_{J=0} + a_2(6p^2)_{J=0} + a_3(6\bar{p}7\bar{p})_{J=0} + a_4(6p7p)_{J=0} \tag{9}$$

and

$$\phi_f = b_1(6\bar{p}7s)_{J=1} + b_2(6p7s)_{J=1} + b_3(6\bar{p}6\bar{d})_{J=1} + b_4(6p6\bar{d})_{J=1} + b_5(6p6d)_{J=1}, \tag{10}$$

with a_1=0.952 56, a_2=−0.278 49, a_3=−0.122 71, a_4=−0.005 139, b_1=0.99 703, b_2=0.053 53, b_3=−0.005 77, b_4=−0.012 06, and b_5=0.053 76 giving an optical oscillator strength of 0.22845. Thus we see that the MCGS wave functions yield oscillator strength in much better agreement with the measured value of 0.21 used to normalize the experimen-

TABLE I. Differential cross sections, in units of 10^{-20} m^2 sr^{-1}, for electron excitation of the $6p7s\ ^3P_1$ state of Pb. The numbers in parentheses are absolute errors.

Angle (deg)	Electron energy					
	10 eV	20 eV	40 eV	60 eV	80 eV	100 eV
1	4.1(1.0)	22.5(5.6)	59(14)	86(20)	109(26)	121(29)
2	3.67(65)	21.0(3.6)	46.6(7.6)	59.3(9.6)	64(10)	61.4(9.9)
3	3.33(51)	18.8(2.8)	33.9(4.9)	37.1(5.3)	33.6(4.8)	28.5(3.7)
4	3.04(45)	16.4(2.3)	23.3(3.2)	22.1(3.0)	17.6(2.4)	13.5(1.7)
5	2.77(40)	13.9(1.9)	15.7(2.1)	13.1(1.7)	9.6(1.3)	6.93(84)
6	2.53(36)	11.6(1.6)	10.7(1.4)	7.9(1.0)	5.48(74)	3.82(46)
7	2.31(33)	9.6(1.3)	7.4(1.0)	4.95(65)	3.24(45)	2.21(26)
8	2.10(29)	8.1(1.1)	5.12(68)	3.24(43)	1.93(27)	1.29(15)
9	1.90(27)	6.87(94)	3.52(47)	2.19(29)	1.13(17)	0.730(91)
10	1.71(24)	5.91(81)	2.36(32)	1.46(20)	0.73(12)	0.514(65)

tal data. Note that both the initial and final states are dominated by a single configuration.

IV. RESULTS AND DISCUSSION

Normalized generalized oscillator strengths for the excitation of the $6p7s\ ^3P_1$ state versus the squared momentum transfer at all energies are shown in Fig. 1. Note that all energies that we have studied, except an electron energy of 10 eV which is at the limit of validity for this normalization technique defined as approximately 2.5 times the excitation energy, are within the applicability of the FSF method. Indeed, the absolute GOS data points corresponding to zero scattering angles terminate on the FSF curve for all energies and this implies that our results are correctly normalized. But, according to the theory [17], GOS values should be fitted by straight lines which terminate on the FSF curve. In our case GOS results do not follow this prediction especially at $E_0 > 20$ eV. This is consistent with the normalization procedure described by Felfli and Msezane [17] where the linear variation of the GOS with K^2 is extensive for E values close to the ω, but it covers fewer and fewer scattering angles as E increase. As one can see from Fig. 1, the normalized GOSs rapidly decrease with increasing momentum transfer at higher electron impact energies. The minimal values of squared momentum transfer (indicated in Fig. 1) slide down the forward scattering function curve as the energy decreases, from 0.0036 at 100 eV to 0.0459 at 10 eV, and this behavior is alsopredicted by theory [17].

The present experimental and theoretical GOSs at (a) $E_0 = 20$ eV and (b) $E_0 = 60$ eV are shown in Fig. 2. We can see that the SCGS results for both energies lie below the MCGS calculations and experimentally obtained GOSs as well. This behavior is expected from the values of the oscillator strengths obtained in the two calculations. It is obvious that there is a good agreement between experiment and MCGS theory especially at 60 eV and scattering angles above 2°.

The experimental DCSs for the $6p7s\ ^3P_1$ excitation from the ground state of lead are tabulated in Table I and shown in Figs. 3 and 4. We compared the measured results with the present MCGS and SCGS calculated values. As one can see, the shapes of the DCS are all the same and are the classical shape of an allowed transition in the forward direction. We

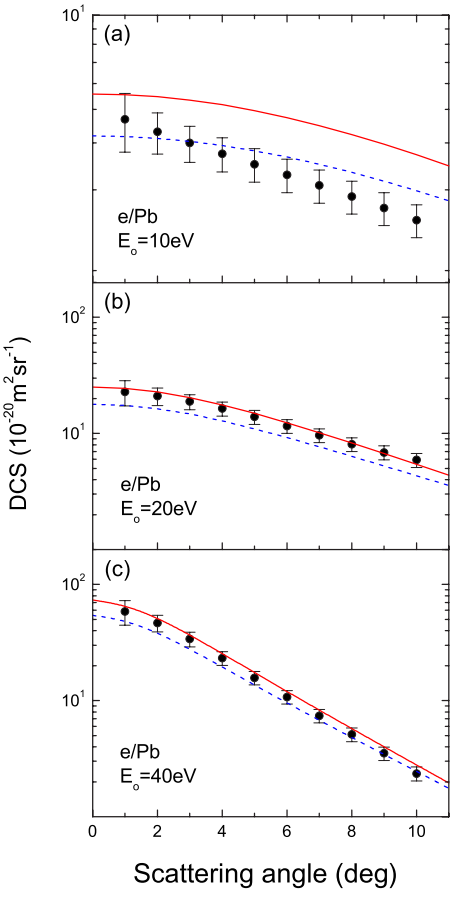

FIG. 3. (Color online) Differential cross sections for the $6p7s\ ^3P_1$ excitation of lead at (a) 10 eV, (b) 20 eV, and (c) 40 eV electron-impact energies. Filled circles with error bars denote the present experimental results. Solid line shows DCSs calculated by the MCGS approximation and the dashed line shows the results obtained using the SCGS approximation.

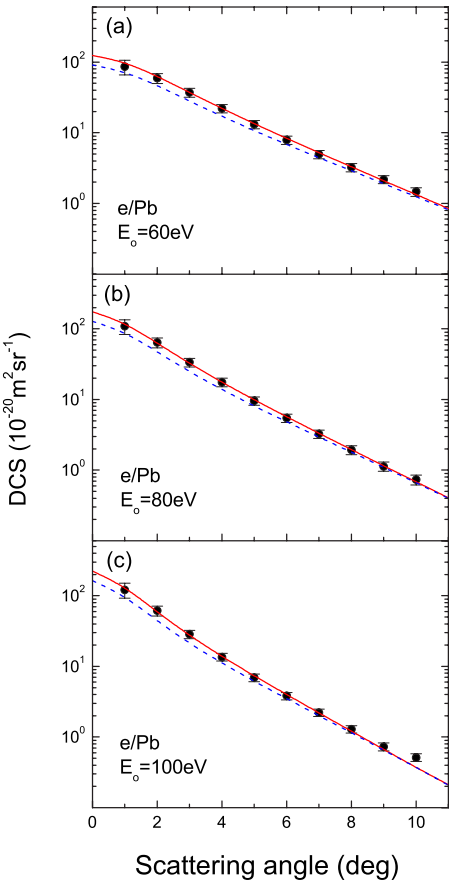

FIG. 4. (Color online) As for Fig. 3 except for (a) 60 eV, (b) 80 eV, and (c) 100 eV electron-impact energies.

find very good agreement, considering both the absolute value and the shape, between our experimental DCSs and our MCGS calculation at all energies over the whole angular range except at the lowest incident energy of $E_0=10$ eV [Fig. 3(a)], where experiment gives smaller DCSs at all scattering angles. This is consistent with the results for the GOS values shown in Fig. 1 and the fact that distorted-wave methods are less reliable at impact energies near threshold. At the same energy, the SCGS results are lower than results obtained using MCGS approximations but good agreement with experiment has been obtained at scattering angles up to 5°. The fact that the SCGS results are in better agreement with the experiment at this energy is fortuitous. The SCGS and MCGS cross sections have very similar shapes at all energies, with the SCGS DCSs consistently smaller. However, as the impact energy increases, the SCGS and MCGS results approach each other and converge to the measured DCSs.

V. CONCLUSIONS

We have presented both experimental and theoretical results for the generalized oscillator strengths and differential cross sections for the excitation of the $6s7p\ ^3P_1$ state of lead in the intermediate electron energy range from 10 to 100 eV and small scattering angles up to 10°. The good agreement between measurement and theory especially at higher electron-impact energies indicate that our results are highly accurate. The obtained data are crucial for normalization and determination of the absolute differential cross section at higher scattering angles and give the basis for a further detailed study of the electron-Pb scattering processes.

ACKNOWLEDGMENTS

This work has been carried out within project 141011 financed by Ministry of Science and Environmental Protection of Republic of Serbia. A.D.S. would like to thank NSERC Canada for financial support.

[1] S. Van Eck, S. Goriely, A. Jorissen, and B. Plez, Nature (London) **412**, 793 (2001).
[2] J. J. Cowan, C. Sneden, J. W. Truran, and D. L. Burris, Astrophys. J. Lett. **460**, L115 (1996).
[3] A. Goswami, W. Aoki, T. C. Beers, N. Christlieb, J. E. Norris, S. G. Ryan, and S. Tsangarides, Mon. Not. R. Astron. Soc. **372**, 343 (2006).
[4] J. A. Cardelli, Science **265**, 209 (1994).
[5] W. Williams and S. Trajmar, J. Phys. B **8**, L50 (1975).
[6] K. Bartschat, J. Phys. B **18**, 2519 (1985).
[7] W. P. Wijesundra, I. P. Grant, and P. H. Norrington, J. Phys. B **25**, 2165 (1992).
[8] S. Kaur, R. Srivastava, R. P. McEachran, and A. D. Stauffer, J. Phys. B **33**, 2539 (2000).
[9] H. Geesmann, M. Bartsch, G. F. Hanne, and J. Kessler, J. Phys. B **24**, 2817 (1991).
[10] C. Herting, G. F. Hanne, K. Bartschat, K. Muktavat, R. Srivastava, and A. D. Stauffer, J. Phys. B **36**, 3877 (2003).
[11] S. Milisavljević, M. Parđovska, D. Šević, V. Pejčev, D. M. Filipović, and B. P. Marinković, in *Proceedings of the 23rd Symposium on Physics of Ionized Gases, Contributed Papers and Abstracts of Invited Lectures, Topical Invited Lectures and Progress Reports*, edited by N. Simonović, B. P. Marinković, and Lj. Hadžievski (Institute of Physics, Belgrade, 2006), p. 55.
[12] B. P. Marinković, V. Pejčev, D. M. Filipović, D. Šević, S. Milisavljević, and B. Predojević, Radiat. Phys. Chem. **76**, 455 (2007).
[13] S. Milisavljević, D. Šević, R. K. Chauhan, V. Pejčev, D. M. Filipović, R. Srivastava, and B. P. Marinković, J. Phys. B **38**, 2371 (2005).
[14] D. V. Fursa, I. Bray, R. Panajotović, D. Šević, V. Pejčev, D. M. Filipović, and B. P. Marinković, Phys. Rev. A **72**, 012706 (2005).
[15] D. M. Filipović, B. Predojević, V. Pejčev, D. Šević, B. P. Marinković, R. Srivastava, and A. D. Stauffer, J. Phys. B **39**, 2583 (2006).
[16] R. T. Brinkmann and S. Trajmar, J. Phys. E **14**, 245 (1981).
[17] Z. Felfli and A. Z. Msezane, J. Phys. B **31**, L165 (1998).
[18] N. B. Avdonina, Z. Felfli, and A. Z. Msezane, J. Phys. B **30**,

2591 (1997).
[19] L. Vušković, S. Trajmar, and D. F. Register, J. Phys. B **15**, 2517 (1982).
[20] Available at http://physics.nist.gov/cgi-bin/ASD/lines1.pl
[21] P. S. Doidge, Spectrochim. Acta, Part B **50**, 209 (1995).
[22] E. Biemont, H. P. Garnir, P. Palmeri, Z. Li, and S. Svanberg, Mon. Not. R. Astron. Soc. **312**, 116 (2000).
[23] R. K. Chauhan, R. Srivastava, and A. D. Stauffer, J. Phys. B **38**, 2385 (2005).
[24] F. A. Parpia, C. Froese Fischer, and I. Grant, Comput. Phys. Commun. **94**, 249 (1996).